Differentiation (2007) DOI: 10.1111/j.1432-0436.2007.00195.x

ORIGINAL ARTICLE

Eleni Hjiantoniou · Mustafa Anayasa · Paschalis Nicolaou · Ioannis Bantounas · Masahiro Saito · Sachiko Iseki · James B. Uney · Leonidas A. Phylactou

Twist induces reversal of myotube formation

Received December 20, 2006; accepted in revised form May 3, 2007

Abstract Mammals possess reduced ability to regenerate lost tissue, compared with other vertebrates, which can regenerate through differentiation of precursor cells or de-differentiation. Mammalian multinucleated myotube formation is a differentiation process, which arises from the fusion of mononucleated myoblasts and is thought to be an irreversible process toward muscle formation. By overexpressing the Twist gene in terminally differentiated myotubes, we managed to induce reversal of cell differentiation. More specifically, following expression of the Twist gene, myotubes underwent morphological changes that caused them to cleave. This was accompanied by a reduction in the expression of certain myogenic markers. Interestingly, Twist overexpression also caused a reduction in the muscle transcription factor MyoD. Further experiments showed an increase in the cell cycle entry molecule, cyclin D1 and initiation of DNA synthesis, due to Twist overexpression. The exploitation of Twist-mediated reversal of differentiation and the study of its specific mechanism would be important in order to study mammalian cellular de-differentiation and determine its potential in muscle regeneration.

Key words twist · myotubes · reversal of differentiation

Eleni Hjiantoniou · Mustafa Anayasa · Paschalis Nicolaou · Leonidas A. Phylactou (✉)
The Cyprus Institute of Neurology & Genetics
P.O. Box 23462, 1683 Nicosia, Cyprus
Tel: +357 22 358600
Fax: +357 22 358237
E-mail: laphylac@cing.ac.cy

Ioannis Bantounas · James B. Uney
The Henry Wellcome Laboratories for Integrative Neuroscience and Endocrinology, Dorothy Hodgkin Building
University of Bristol, Whitson Street
Bristol BS1 3NY, U.K.

Masahiro Saito
Department of Molecular and Cellular Biochemistry
Osaka University
Graduate School of Dentistry
Yamadaoka 1-8
Suita City
Osaka 565-0871
Japan

Sachiko Iseki
Section of Molecular Craniofacial Embryology
Graduate School, Tokyo Medical and Dental University
1-5-45 Yushima, Bunkyo-ku, Tokyo 113-8549, Japan

Introduction

While vertebrates like salamanders, zebrafish, and *Xenopus laevis* have developed advanced regenerative abilities, mainly through differentiation of precursor cells or de-differentiation, mammals have a limited capacity to regenerate (Odelberg et al., 2000). Differentiation of mammalian cells is thought to be a terminal and irreversible process. The *in vitro* differentiation of myocytes into myotubes is a well-characterized example of terminal differentiation (Andres and Walsh, 1996; Sers et al., 1997). Myoblasts are skeletal muscle cells that are capable of cell proliferation in the presence of growth factors. They could also enter terminal differentiation when grown to confluency and deprived of growth factors. Differentiated cells fuse to form multinucleated myotubes in an irreversible procedure. Currently, there is very little evidence for mammalian cellular reversal of differentiation. Researchers, however, have been trying to induce de-differentiation in mammalian cells, mostly *in vitro*. Because it forms a good model, most of the previous experiments to study myotube de-differentiation were carried out in the mouse C2C12 cell line. When newt and mouse myoblasts were allowed to fuse together

in vitro both cell nuclei could re-enter the cell cycle by responding to thrombin and serum (Kumar et al., 2004). Another study showed that newt extracts could induce mouse myotubes to reinitiate the cell cycle (McGann et al., 2001). Overexpression of the Msx-1 gene in myotubes caused their cleavage into proliferating mononucleated cells, which could trans-differentiate into other cell types (Odelberg et al., 2000). Myoseverin, a trisubstituted purine, also caused mammalian myotube de-differentiation (Rosania et al., 2000). Recently, introduction of the CSX/Nkx2.5 transcription factor caused a change of morphology of myotubes and cleavage into smaller parts but without any apparent cell cycle activity (Riazi et al., 2005). The exact mechanism of induced de-differentiation and its *in vivo* potential however remains yet to be seen. Mammalian de-differentiation is a new research field that will provide additional basic knowledge about mechanisms of mammalian regeneration. The identification of molecules, which can induce or are involved in de-differentiation, is of vital importance (Echeverri and Tanaka, 2002).

Twist is a nuclear basic helix-loop-helix (bHLH) transcription factor, crucial for mesoderm formation in *Drosophila* (Thisse et al., 1988). The HLH motif was first identified in the murine DNA-binding proteins E12 and E47 (Murre et al., 1989). In mammals, Twist is mostly expressed in cranial neural crest derivatives and in mesenchymal structures (Bate et al., 1991; Hebrok et al., 1994; Fuchtbauer, 1995; Gitelman, 1997) and its expression has been implicated in the inhibition of differentiation of several mesodermal cell lineages, including muscle (Hebrok et al., 1994; Spicer et al., 1996), cartilage (Poliard et al., 1995), and bone (Murray et al., 1992; Lee et al., 1999). Mutations in the TWIST gene are responsible for the Saethre-Chotzen syndrome, an autosomal dominant craniosynostosis characterized by abnormal fusion of the cranial sutures (el Ghouzzi et al., 1997; Howard et al., 1997). bHLH proteins bind as dimers to a consensus sequence E-box through their basic domain (Ephrussi et al., 1985). Several experiments indicate that the Twist family members bind preferentially to the E-box of MyoD/E heterodimers, as homodimers (Lee et al., 1999; Kophengnavong et al., 2000) or heterodimers (Spicer et al., 1996) with the E protein family. Moreover, the basic domain of murine Twist has been reported to physically interact with the basic domain of MyoD (Hamamori et al., 1997). The association between these basic regions is implicated as one mechanism by which Twist can regulate myogenesis in vertebrates.

Apart from its role in control of cell differentiation, Twist has been found to be involved in cancer. Overexpression of Twist has been reported in several types of cancer, including invasive lobular breast carcinomas (Yang et al., 2004), T-cell lymphomas (van Doorn et al., 2004), and rhabdomyosarcomas (Maestro et al., 1999). Finally, a role for Twist in programmed cell death has been revealed. It has been reported that Twist antagonizes p53-dependent apoptosis and growth arrest (Maestro et al., 1999) and that Twist overexpression is associated with acquired drug resistance in human cancer cells (Wang et al., 2004). Moreover, it has been shown that Twist is involved in insulin-like growth factor-1 (IGF-1) receptor-mediated protection and modulation of tumor necrosis factor-α (TNF-α)-dependent apoptosis (Dupont et al., 2001) and that by using artificial catalytic DNA molecules (DNazymes), down-regulation of Twist gene expression increases cellular apoptosis (Hjiantoniou et al., 2003).

In this paper, we show yet another novel and important aspect of the Twist function. We show that overexpression of the Twist gene in differentiated mouse muscle cells induces reversal of muscle differentiation.

Methods

Cloning and generation of recombinant adenovirus constructs

Mouse Twist cDNA and a control sequence (an inactive hammerhead ribozyme against Twist RNA that has been shown not to cause any reduction in Twist RNA, protein levels—data not shown) were cloned in vectors for adenoviral production. Recombinant E1-deleted adenoviral constructs were produced as described before (Glover et al., 2002).

Tissue culture

C2C12 mouse myoblasts were grown to confluency in growth media (GM), Dulbecco modified eagle's medium (DMEM) with 10% fetal bovine serum (FBS) and 2 mM glutamine (Invitrogen, Carlsbad, CA). They were then switched to differentiation media (DM), DMEM, 4% Horse Serum, and 2 mM glutamine for up to 4 days for myotube formation. For adenoviral transfections, 50 MOI were incubated with myoblasts for inhibition of differentiation or with myotubes for de-differentiation studies for 48 hr in DM. Transfected and untransfected myotubes were incubated further in GM or split by gentle trypsinization (0.25% trypsin/1 mM ethylene diamine tetraacetic acid [EDTA]) and transferred to 60 mm plates coated in 0.75% gelatin (Sigma, St. Louis, MO) in DM at a density of 1–2 myotubes/mm^2. In the case of split cells, the following day, carried-over myoblasts were killed by pipette tip ablation and the media was replaced by fresh DM for another 24 hr. Myotubes were then incubated with GM, marked, and digital images taken under an inverted microscope (Nikon TE2000E, Nikon, Japan) or processed for other studies. Two hundred and fifty to 350 myotubes were evaluated for each experiment.

RNA analysis

Total RNA was extracted from transfected or untransfected myotubes (Perfect RNA Eukaryotic Mini kit, Eppendorf, Germany) and subjected to reverse transcription. For detection of the Twist RNA in myotubes by polymerase chain reaction (PCR), Twist (fwd 5′-CCCAAGCTTGTCGTACGAGGAGCTGCAGA-3′, rev 5′-CGCGGATCCCTCCAGACGGAGAAGGCGTA-3′) primers were used under quantitative conditions. For detection of molecular changes by RT/PCR, following transfections, MyoD (fwd 5′-CCCGCGCTCCAACTGCTCTGAT-3, rev 5′-CCTACGGTGGT GCGCCCTCTGC-3′), cdk4 (fwd 5′-CAGCACTCCTACCTG

CACAA-3′, rev 5′-AGGAGAGGTGGGGACTTGTT-3′), cycD1 (fwd 5′-GGCACCTGGATTGTTCTGTT-3′, rev 5′-CAGCTT GCTAGGGAACTTGG-3′), MEF2 (fwd 5′-GAATGCCCAA AGGATAAGCA-3′, rev 5′-TGTCCTAGATGGTGCTGCTG-3′), and glyceraldehyde-3-phosphate dehydrogenase (GAPDH) primers (fwd 5′-TCATCATCTCCGCCCCTTCC-3′ and rev 5′-GAG-GGGCCATCCACAGTCTT-3′) primers were used after determining quantitative conditions (27, 27, 28, 26, and 25 cycles, respectively). For quantitative studies, experiments were repeated at least six times and gel bands were measured using Scion Image software.

Western blotting

Twenty to 30 μg of protein extracts were incubated with the Twist antibody (1:200) or caspase-3 antibody (1:7,000, Santa Cruz, Santa Cruz, CA) followed by incubation with a goat anti-mouse immunoglobulin G (IgG) or donkey anti-rabbit secondary antibodies, respectively, conjugated to horseradish peroxidase (Santa Cruz).

Immunofluorescent studies

Myotubes were incubated with various antibodies after 0–3 days of GM induction. Briefly, cells were fixed in 4% paraformaldehyde and blocked in 1% Triton X-100 dissolved in 1% bovine serum albumin (BSA) in phosphate-buffered saline (PBS). Myotubes were then exposed to myosin heavy chain (MHC) (MY32 Sigma 1:400), myogenin (1:200, Santa-Cruz), MyoD (1:100 Pharmingen, San Diego, CA), and Twist (1:400) antibodies for 1 hr at 37°C and then incubated with the following secondary antibodies: a goat anti-mouse Texas Red, a goat anti-rabbit Texas Red, and a goat anti-mouse fluorescein isothiocyanate (FITC) antibody (Jackson Immunoresearch, West Grove, PA) for 30 min at room temperature and nuclei were stained with 4,6-diamidino-2-phenylindole (DAPI) (Vysis, Downers Grove, IL). Cells were visualized under a Nikon Eclipse 2000 inverted microscope, images acquired by DXM1200F digital camera (Nikon), and analyzed by Adobe Photoshop software.

Cell cycle studies

Myotubes incubated in GM up to 2 days were then supplemented with 50 μM bromodeoxyuridine (BrdU) (Sigma) for a further 24 hr, followed by fixation at room temperature. Cells were then permealized as described above. The cells were then denatured with 2N HCl for 30 min at 37°C and then blocked in 1% BSA in PBS for 10 min. Myotubes were then exposed to anti-BrdU mouse antibody (Sigma) for 1 hr at 37°C and then after washing with PBS were exposed to a goat anti-mouse secondary antibody for 30 min at room temperature.

DNA analysis for apoptosis

DNA extractions were carried out using the DNeasy Tissue Kit (Qiagen, Germany) and then concentrated in the SpeedVac Concentrator (Savant SVC100H, Savant, Rochester, NY). Equal amounts of DNA samples were loaded on 1.8% agarose gel. The DNA was visualized by ultraviolet (UV) illumination.

Results

An E1-deleted adenovirus, carrying the mouse Twist cDNA (AdT), was constructed. Twist is known to inhibit myogenesis (Hebrok et al., 1994); hence, in order to determine whether AdT produced functional Twist, C2C12 myoblasts were transduced with the recombinant virus. A control adenovirus (AdC), expressing an inactive hammerhead ribozyme sequence, was also used.

Following transfections, myoblasts were induced to become multinucleated myotubes with differentiation medium. There was a marked inhibition of myogenesis in cells transfected with the AdT, compared with AdC-transfected and untransfected myoblasts, which fused normally into myotubes (Fig. 1A).

Having shown that the AdT viral vector can transduce mouse myoblasts and inhibit the formation of multinucleated myotubes, its efficiency to transfect already formed myotubes was checked at the RNA and protein levels (Figs. 1B,1C). Overproduction of Twist mRNA was detected in C2C12 myotubes transfected with the AdT viral vector whereas control-transduced cells (AdC) showed no increase in Twist mRNA levels compared with the endogenous levels (Fig. 1B). Moreover, Western blot analysis detected overexpression of Twist protein (Fig. 1C), compared with untransfected cells or cells transfected with the control adenovirus (AdC) with a Twist antibody, which is known to detect only transgene Twist product (unpublished data).

Three days after the transfection with the Twist-expressing adenoviral vector, there were fewer myotubes present compared with the untransfected or with those transfected with the AdC (Fig. 2A). Overexpression of the Twist gene in terminally differentiated myotubes seemed to have caused their elimination from the culture.

In order to clarify and characterize in more detail the effect of the overexpression of the Twist gene on multinucleated myotubes, a method was developed similar to the one reported before (Odelberg et al., 2000) to isolate individual myotubes. By using a specific protocol in which differentiated cells were detached from the cultured plate and separated from the myoblasts, individual myotubes were observed under a microscope over a period of time. A significant proportion of myotubes transfected with the AdT viral vector (28%) underwent cleavage (Figs. 2B,2C). At the beginning myotube structure was distorted, followed by the cleavage into smaller cellular parts. This occurred mainly in two ways: cleavage was around the areas where the nuclei reside (Fig. 2B) and cleavage took place in the middle of the myotube, following separation of the nuclei into the two cellular halves (Fig. 2C). No cleavage was seen in any of the untransfected myotubes (Fig. 2D) or in myotubes transfected with the control virus, AdC (Fig. 2E), indicating the specificity of cleavage by Twist. Since fusion of myoblasts is the procedure that forms multinucleated myotubes, these results indicate that overexpression of the Twist gene might be inducing reversal of cell differentiation.

The results described above indicate that the overexpression of the Twist gene induces myotubes to undergo

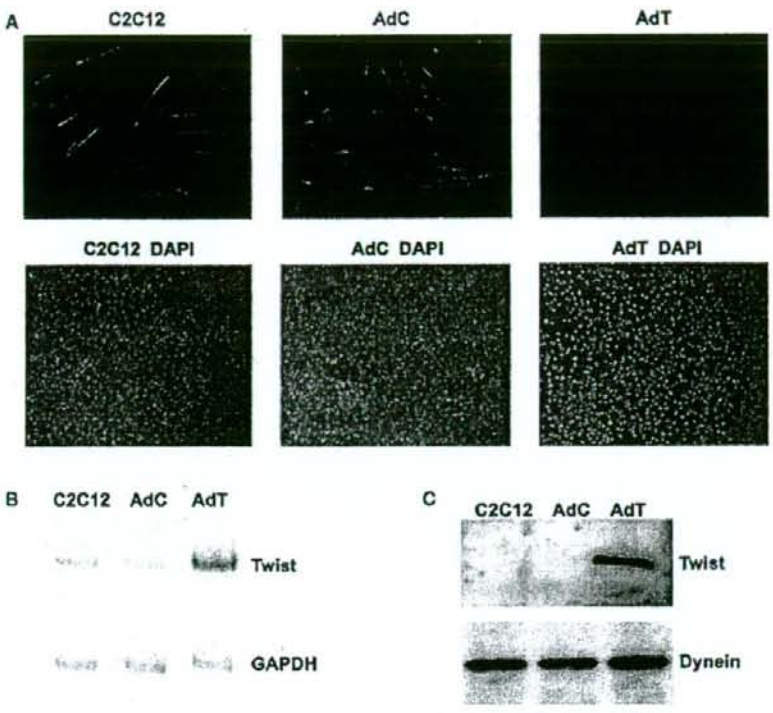

Fig. 1 Twist inhibits myotube formation and is overexpressed in myotubes. (**A**) C2C12 myoblasts were transfected with a Twist-expressing adenovirus (AdT) or a control adenovirus (AdC) and were induced to differentiate for 3 days as shown by MHC immunostaining and nuclear staining by DAPI. Whereas both AdC tranfected and untransfected C2C12 cells readily formed myotubes, overexpression of Twist cDNA did not. Transfection of AdT in mouse myotubes caused an overexpression of the Twist cDNA (AdT) as detected by RT/PCR (**B**) and Western blotting (**C**), compared with control-transfected cells (AdC) and untransfected cells. DAPI, 4,6-diamidino-2-phenylindole; PCR, polymerase chain reaction; MHC, myosin heavy chain.

structural changes leading to their cleavage. Myotube formation is always accompanied by an increase of several myogenic markers and the termination of cell cycle (Tajbakhsh, 2005). Since the overexpression of the mouse Twist cDNA showed signs of cell differentiation reversal, as a next step the levels of an early and a late myogenic marker were investigated.

Immunodetection of the MHC, a late marker of myogenesis, revealed a heavy reduction in the expression of the MHC gene. The decrease was very pronounced 3 days after the transfection of the viral vector AdT (Fig. 3A). Normal staining was observed in untransfected cells or in cells transfected with the control viral vector AdC. Moreover, nuclear staining of the cells transfected with the AdT viral vector shows areas where the nuclei are clustered in the two ends of the myotube, presumably before cleavage, which was also demonstrated in Figure 2C. In order to perform a more detailed analysis, immunodetection of MHC and also of myogenin (an early marker of myogenesis) was performed on individual myotubes. Following transfection with the Twist-expressing adenovirus (AdT), immmunodetection revealed a reduction in the expression of myogenin and MHC, whereas untransfected cells or cell transfected with the control viral vector AdC maintained their normal myogenin and MHC levels (Fig. 3B). In an attempt to quantitate the effect of Twist on both these proteins whose levels are high during the process of differentiation, myotubes that did not stain for myogenin or MHC were counted 2 and 3 days after the introduction of GM to the cells (Fig. 3C). Both levels of myogenin and MHC showed a dramatic reduction in the myotubes transfected with the Twist cDNA with an increasing trend over time. Because both these molecules are involved during muscle cell differentiation and the induction of their gene expression accompanies muscle formation, these results imply that among other things, Twist overexpression in multinucleated myotubes causes reduction of proteins that are involved in myogenesis.

Having seen a reduction in the markers of muscle formation and cleavage of differentiated myotubes, resembling reversal of differentiation, experiments were continued in order to investigate whether cell cycle re-

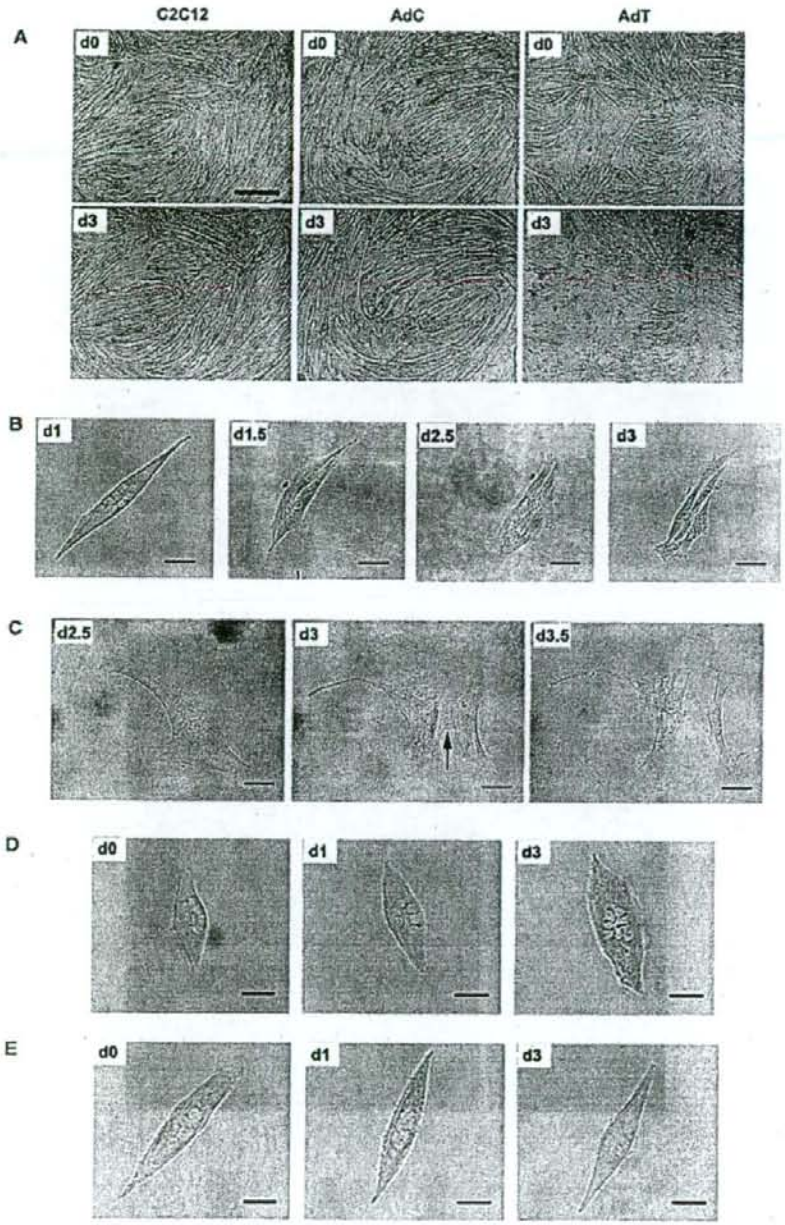

Fig. 2 Twist overexpression caused morphological changes in myotubes. (**A**) Following muscle cell differentiation for 4 days (d0), cells were transfected with the Twist-expressing virus (AdT), the control virus (AdC) for 2 days and then incubated for 24 hr (d3) in growth medium. AdT transfection caused a reduction of myotubes. (**B**) Twist overexpression causes cleavage of individual multinucleated myotubes in mainly two ways. Following AdT transfection and incubation in GM, the myotube (d1) was torn and cleaved around the nuclei (d1.5–d3). (**C**) In the second way, myotubes were cleaved in the middle (indicated by an arrow), following the separation of the nuclei in the two cellular halves. No cleavage was seen in untransfected (C2C12) (**D**) and control-transfected myotubes (AdC) (**E**). Scale bars represent 0.05 cm. GM, growth medium.

activation takes place. This was carried out by detecting possible changes in molecules that play a key role in this process. One of the myogenic regulatory factors, MyoD, a transcription factor, up-regulated during the exit of muscle cells from the cell cycle and induced during myogenesis, was chosen as a first target. MyoD RNA levels were substantially reduced in cells transfected with the overexpressing Twist adenoviral vector

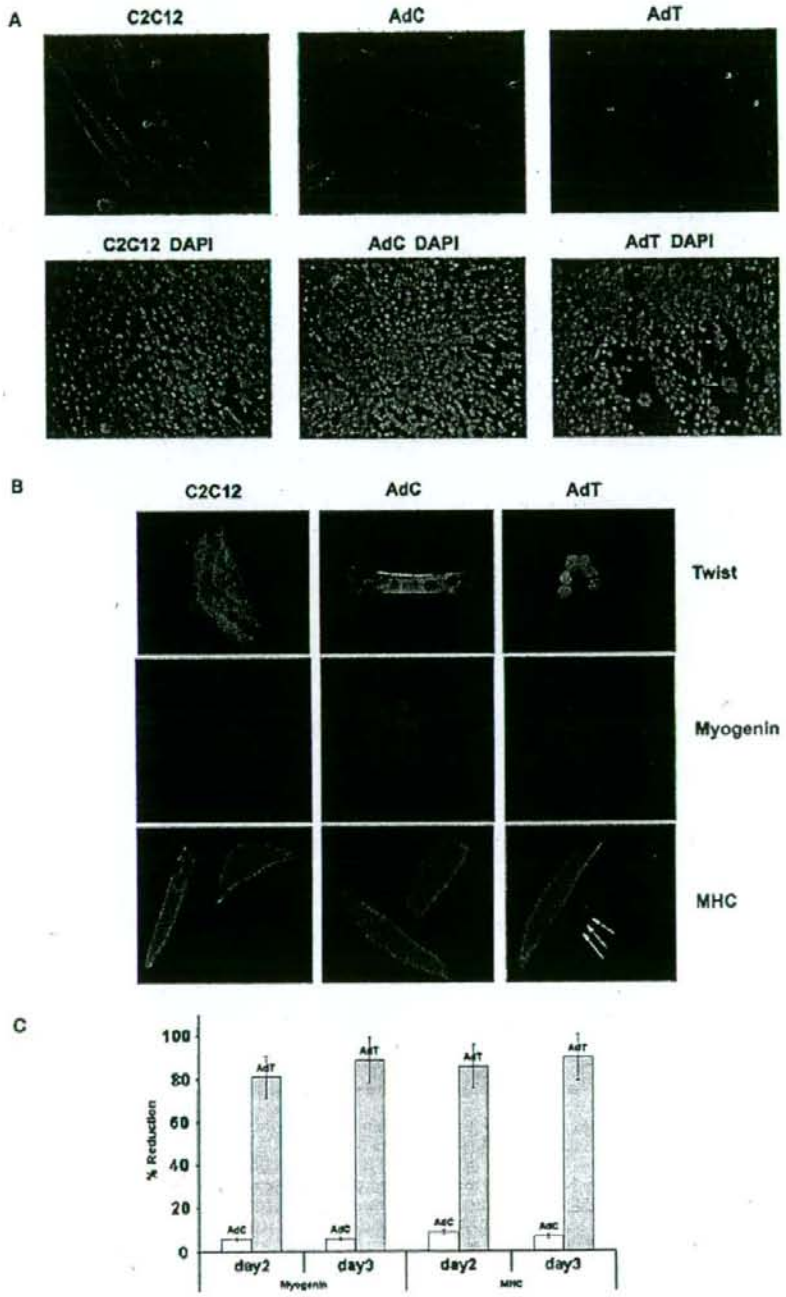

(Fig. 4A). It was found that MyoD levels in cells transfected with the Twist gene were more than 50% lower than the control cells (Fig. 4D). Moreover, immunocytochemistry experiments were performed to determine MyoD protein levels in Twist-transfected cells. Similar to the RNA levels, MyoD protein levels were reduced (Fig. 4B). Proper MyoD staining was observed in cells transduced with the control AdC viral vector and in untransfected cells. These results show that overexpression of the Twist gene has a negative effect on the expression of the MyoD, which is a known important factor for myogenesis to happen. Because MyoD reduction levels were found reduced following the overexpression of the Twist gene, various other molecules involved in cell cycle and differentiation were checked. Cyclins and cyclin-dependent kinases (cdks) form complexes and control several key points of the cell cycle. The RNA levels of Cyclin D1, which is usually involved in the first steps of cell cycle activation, were found elevated only in cells transfected with the AdT (Figs. 4C,4D). No significant changes were seen in its partner cdk4 and MEF2, the molecule that conjugates with MyoD during myogenesis (Fig. 4C). Therefore, these results have provided evidence about the reactivation of the cell cycle following the expression of the Twist gene in the terminal differentiated mouse myotubes. This evidence comes from the gene expression changes detected in molecules involved in myogenesis and in the cell cycle.

In order to exclude the possibility that Twist induces apoptosis or necrosis in transfected myotubes, two assays were performed to determine whether this happens. A DNA (ethidium bromide) assay (early apoptosis step) and a Western blot to detect caspase levels, known to be increased during apoptosis (late apoptosis step), were carried out (Figs. 4E,4F). Ethidium bromide assay showed no DNA fragmentation and the smear observed, which denotes some necrosis in the myotubes, was similar between the Twist-transduced cells (AdT) and the control-transduced cells (AdC) and was less in the untransfected C2C12 cells. This is probably necrosis due to the transduction of viral vectors, which is added to the known minor necrosis observed in differentiated muscle cells (Shiokawa et al., 2002). Moreover, Western blot analysis showed no caspase-induced apoptosis, in cells transfected with the Twist viral vector (AdT), compared with untransfected C2C12 cells or cells transfected with the control viral vector (AdC), indicating that Twist does not cause early or late apoptosis to the transduced myotubes. This agrees with other reports which showed that Twist not only causes apoptosis but can also act as an anti-apoptotic molecule (Maestro et al., 1999; Hjiantoniou et al., 2003; Demontis et al., 2006).

Since DNA synthesis is the first step in cell cycle activation, further experiments were performed in order to observe such events in myotubes transfected with the AdT viral vector. For this purpose, Twist-transfected cells were incubated with BrdU. Immunostaining revealed that there was an initiation of DNA synthesis, compared with untransfected or AdC-transfected cells, which remained outside the cell cycle (Fig. 5A). In order to investigate in more detail the initiation of DNA synthesis coupled to the reduction of muscle cell markers MyoD, myogenin, and MHC, triple immunocytochemistry experiments were carried out (Figs. 5B–5D). These experiments reconfirmed that Twist expression causes reduction in the levels of all three molecules (MyoD, myogenin, and MHC) accompanied by the active DNA replication in those cells (Fig. 5B). However, it was interesting to observe that at an earlier stage the Twist expression could only induce a reduction in the levels of myogenic molecules but not in DNA synthesis (Fig. 5C). These results imply that although cells enter the cycle, this happens at a relatively later stage. Positive staining for the three myogenic markers and absence of BrdU staining was observed in untransfected cells (Fig. 5D) and cells transfected with the control adenoviral vector, AdC (data not shown). Finally, triple immunocytochemistry experiments revealed cleaved cells with positive BrdU staining following transfection with the AdT Twist adenoviral vector (Fig. 5E). Moreover, these cells were negative for MyoD and MHC molecules.

Discussion

These results show that the overexpression of the Twist gene in terminally differentiated muscle cells (myotubes) can re-activate those cells and induce the reversal of

Fig. 3 Reversal of muscle differentiation markers. (**A**) Following myotube differentiation for 4 days, cells were transfected with the Twist-expressing virus (AdT), the control virus (AdC) for 2 days and then incubated for 24 hr (d3) in growth medium. Myotubes were fixed and stained with an MHC antibody and marked with DAPI. White arrows indicate the clustering of the nuclei in the two ends of the myotube, in AdT-transfected cells. (**B**) Myotubes expressing the Twist cDNA via the AdT viral vector caused a reduction in myogenin and MHC muscle differentiation markers, as detected by immunohistochemistry, compared with untransfected (C2C12) and control-transfected individual cells (AdC). Negative staining for myogenin is demonstrated with the absence of nuclear staining, whereas background MHC levels demonstrate negative staining for MHC. (Note that the MHC immunofluorescence images had to be overexposed in order to see a negatively stained myotube, as shown by the arrows.) (**C**) In order to get a quantitation for myogenin and MHC on the negatively stained cells by immunofluorescence, cells were counted and then calculated as a proportion of the untransfected cells. MHC, myosin heavy chain; DAPI, 4,6-diamidino-2-phenylindole.

their differentiation. These myotubes change morphology and eventually cleave into smaller cell products. This cellular cleavage was accompanied by a reduction in early and late markers of muscle differentiation followed by re-activation of the DNA machinery as detected by BrdU incorporation. Regarding the mechanism of the Twist-induced reversal of muscle cell differentiation, the myogenic transcription factor,

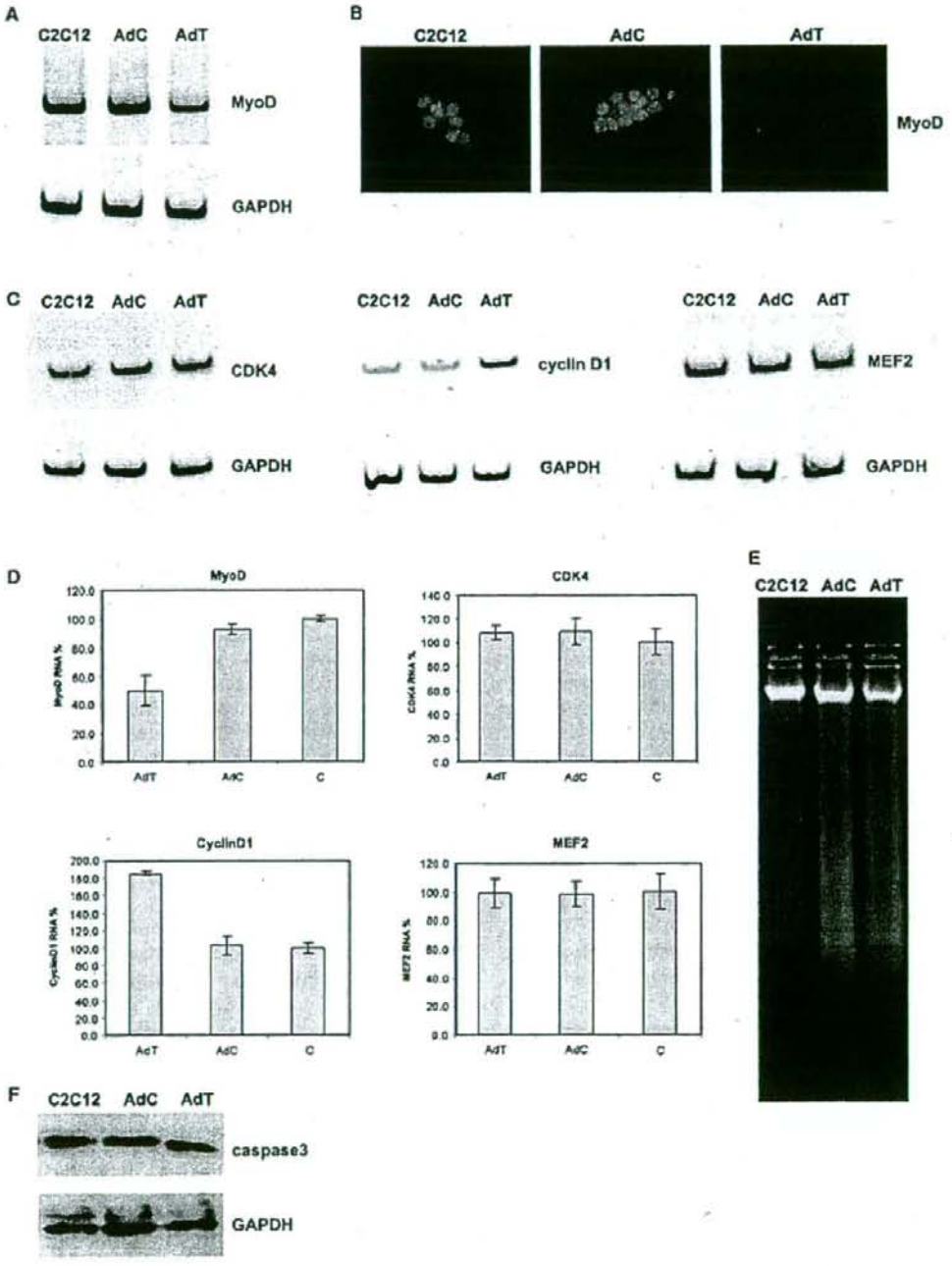

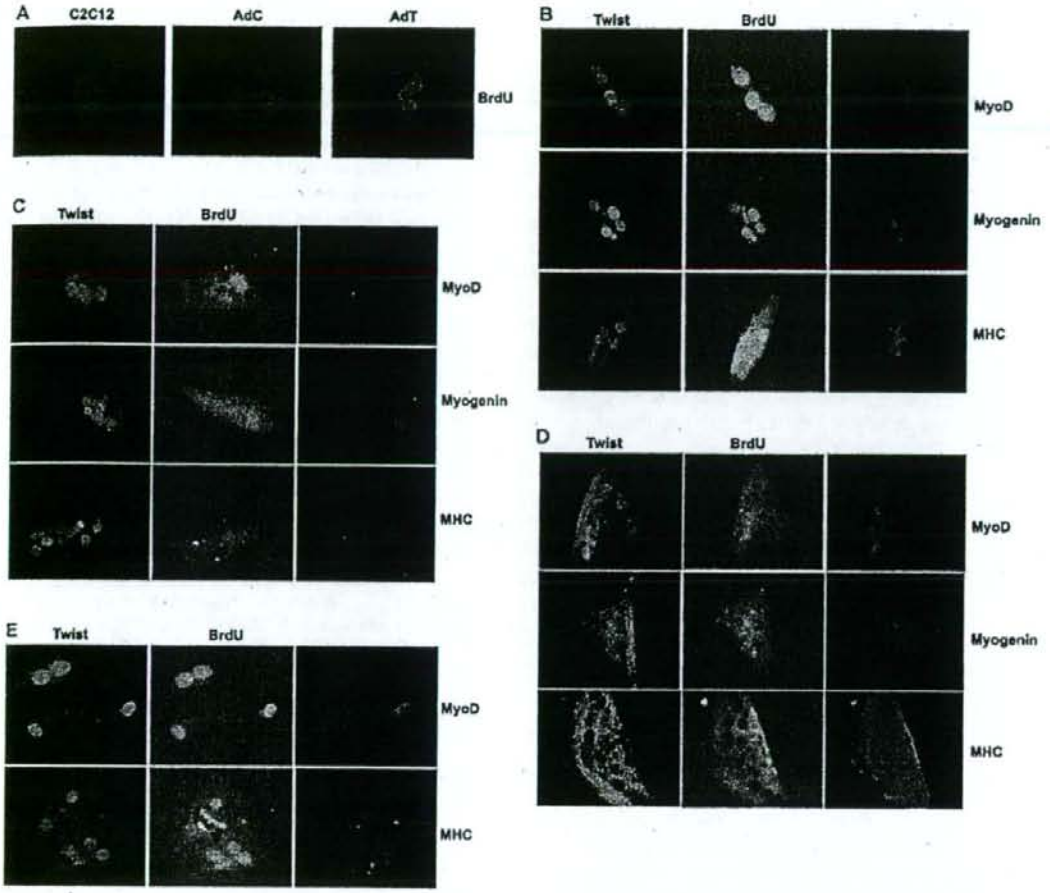

Fig. 5 Reduction of myogenic markers MyoD, myogenin, and MHC followed by re-entry to the cell cycle and accompanied by myotube cleavage. (**A**) Overexpression of the Twist cDNA (AdT) caused an increase in BrdU-positive cells as shown with the intense nuclear coloring compared with untransfected (C2C12) and control-transfected cells (AdC). (**B**) Reduction of myogenic markers MyoD, myogenin, and MHC occurred after transfection of myotubes with the AdT viral vector, as detected by triple immunocytochemistry, coupled with BrdU activity, 3 days after induction with growth medium (GM). (**C**) Only 2 days in GM, AdT-transfected cells demonstrated reduced staining for the myogenic factors MyoD, myogenin, and MHC but were negative for BrdU. (**D**) Untransfected (Twist negative) myotubes demonstrated no BrdU activity and expressed normal MyoD, myogenin, and MHC, as expected. (**E**) Examples of Twist-transfected with active cell cycle (BrdU) and reduced myogenic markers (MyoD, MHC) that underwent cleavage. GAPDH, glyceraldehyde-3-phosphate dehydrogenase; MHC, myosin heavy chain; BrdU, bromodeoxyuridine.

Fig. 4 Twist overexpression targets molecules of muscle cell differentiation and the cell cycle. (**A**) RT/PCR analysis revealed a substantial reduction at the RNA levels of MyoD in cells transfected with the Twist adenovirus (AdT) compared with the control adenovirus (AdC) and untransfected C2C12 cells. (**B**) Twist overexpression (AdT) caused reduction at the MyoD protein levels compared ewith control experiments (C2C12, AdC). (**C**) Investigation at the RNA levels of cdk4, cyclin D1, and MEF2 after overexpressing the Twist gene (AdT) in differentiated myotubes in comparison with control cells (C2C12, AdC). Twist overexpression caused a substantial increase in the levels of cyclin D1 but did not have significant effect on the cdk4 and MEF2. GAPDH was used as an internal control. (**D**) Summary of the RNA quantitation analysis. Values were obtained as ratios of the RNA of interest over the GAPDH internal control. (**E**) DNA apoptotic assay by ethidium bromide showed no fragmentation in Twist-transduced cells (AdT) and similar necrotic smear to the control-transduced cells (AdC), which was slightly higher to the usual necrosis observed in the C2C12 myotubes. (**F**) Western blot analysis showed that the capsase-3 levels in Twist-transduced cells (AdT) were similar to those in control-transduced cells (AdC) and untransfected C2C12 cells. GAPDH, glyceraldehyde-3-phosphate dehydrogenase; PCR, polymerase chain reaction.

MyoD seems to play a major role in this since both its RNA and protein levels have been found to be noticeably reduced. Moreover, cell cycle entry control molecule cyclin D1 was shown to be substantially increased in those cells.

Cellular de-differentiation of muscle is not a natural phenomenon observed in mammalian cells. Terminally differentiated mouse myotubes are incapable of re-entering the cell cycle. The above results provide strong evidence that Twist, a transcription factor known to inhibit differentiation of several cell types, can reverse differentiation, re-initiate cell cycle, and cause cleavage of myotubes when overexpressed in differentiated myotubes. This paper provides some insights into the mechanism of Twist-induced myotube de-differentiation too. Following the expression of the exogenous mouse Twist cDNA, a significant number of cells changed morphology, followed by their cleavage.

Immunofluorescence experiments revealed that myogenic factors are reduced upon expression of the adenovirally delivered mouse Twist cDNA in the presence of growth factors. Entry to the cell cycle was observed at a later stage, which was then followed by myotube cleavage.

Molecular analysis performed revealed that MyoD and cyclin D1 were reduced in cells transfected with Twist-adenoviral vector. MyoD is one of the key transcription factors responsible for the differentiation of myoblasts and for inducing myogenesis by regulating the expression of several genes (Wei and Paterson, 2001). It is known that Twist inhibits the action of MyoD, which subsequently inhibits the differentiation of myoblasts into myotubes. This is a known mechanism in which Twist controls muscle cell differentiation (Spicer et al., 1996; Lee et al., 1999; Kophengnavong et al., 2000). Our experiments show that it may well be possible that Twist inhibits MyoD also from this site. Because MyoD is vital during myogenesis, its levels are high when myotubes are formed. Although Twist and MyoD are co-expressed in myoblasts, Twist might be causing a reduction of MyoD as it is overexpresed at a different time than MyoD. As a result there is a retreat in the differentiation, which leads to the structural changes and the reduction in the late and early markers of myogenesis (MHC and myogenin, respectively). MEF2, the partner of MyoD, which exerts effects on the various gene expression targets, was not found reduced. This might imply that Twist inhibits MyoD directly and not indirectly through another pathway. Our experiments also reveal re-activation of the cell cycle, as seen by the DNA synthesis through the BrdU incorporation. This seems to be supported from the substantially increased cyclin D1 levels in cells transfected with the AdT viral vector. Cyclin D1 coupled with the cdk4 form a complex, which then phosphorylates other proteins, thus promoting the initiation of the cycle (Wei and Paterson, 2001). Cdk4 RNA levels were not found changed in cells transduced with the AdT virus. This was an expected result since cdk4 levels are usually constant during the cell cycle and formation of the cyclinD1/cdk4 complex depends on the availability of cyclin D1. Finally, apoptosis experiments showed that overexpression of the Twist gene does not cause apoptosis in the transduced myotubes (Figs. 4E,4F). Previous reports have demonstrated that Twist might act to prevent apoptosis (Maestro et al., 1999; Hjiantoniou et al., 2003; Demontis et al., 2006).

These results point to a mechanism whereby Twist is acting in a pathway by down-regulating the expression of myogenic factors, which usually differentiate terminally myoblasts into myotubes. This in turn gives signal for the re-entry of cells into the cell cycle and their cleavage.

Future experiments will investigate in more detail the specific mechanism by which Twist causes the reversal of differentiation of myotubes in C2C12 and primary cells and also *in vivo*. Finally, the exploitation of the Twist-mediated de-differentiation pathway should provide insights to possible muscle regeneration pathways.

Acknowledgment This work has been supported by the A.G. Leventis Foundation (grant to L. A. P.) and the Cyprus Research Promotion Foundation (grant to L. A. P.).

References

Andres, V. and Walsh, K. (1996) Myogenin expression, cell cycle withdrawal, and phenotypic differentiation are temporally separable events that precede cell fusion upon myogenesis. J Cell Biol 132:657–666.

Bate, M., Rushton, E. and Currie, D.A. (1991) Cells with persistent twist expression are the embryonic precursors of adult muscles in Drosophila. Development 113:79–89.

Demontis, S., Rigo, C., Piccinin, S., Mizzau, M., Sonego, M., Fabris, M., Brancolini, C. and Maestro, R. (2006) Twist is substrate for caspase cleavage and proteasome-mediated degradation. Cell Death Differ 13:335–345.

Dupont, J., Fernandez, A.M., Glackin, C.A., Helman, L. and LeRoith, D. (2001) Insulin-like growth factor 1 (IGF-1)-induced twist expression is involved in the anti-apoptotic effects of the IGF-1 receptor. J Biol Chem 276:26699–26707.

Echeverri, K. and Tanaka, E.M. (2002) Mechanisms of muscle dedifferentiation during regeneration. Semin Cell Dev Biol 13:353–360.

el Ghouzzi, V., Le Merrer, M., Perrin-Schmitt, F., Lajeunie, E., Benit, P., Renier, D., Bourgeois, P., Bolcato-Bellemin, A.L., Munnich, A. and Bonaventure, J. (1997) Mutations of the TWIST gene in the Saethre-Chotzen syndrome. Nat Genet 15:42–46.

Ephrussi, A., Church, G.M., Tonegawa, S. and Gilbert, W. (1985) B lineage-specific interactions of an immunoglobulin enhancer with cellular factors in vivo. Science 227:134–140.

Fuchtbauer, E.M. (1995) Expression of M-twist during postimplantation development of the mouse. Dev Dyn 204:316–322.

Gitelman, I. (1997) Twist protein in mouse embryogenesis. Dev Biol 189:205–214.

Glover, C.P., Bienemann, A.S., Heywood, D.J., Cosgrave, A.S. and Uney, J.B. (2002) Adenoviral-mediated, high-level, cell-specific transgene expression: a SYN1-WPRE cassette mediates increased

transgene expression with no loss of neuron specificity. Mol Ther 5:509–516.
Hamamori, Y., Wu, H.Y., Sartorelli, V. and Kedes, L. (1997) The basic domain of myogenic basic helix-loop-helix (bHLH) proteins is the novel target for direct inhibition by another bHLH protein, Twist. Mol Cell Biol 17:6563–6573.
Hebrok, M., Wertz, K. and Fuchtbauer, E.M. (1994) M-twist is an inhibitor of muscle differentiation. Dev Biol 165:537–544.
Hjiantoniou, E., Iseki, S., Uney, J.B. and Phylactou, L.A. (2003) DNazyme-mediated cleavage of Twist transcripts and increase in cellular apoptosis. Biochem Biophys Res Commun 300:178–181.
Howard, T.D., Paznekas, W.A., Green, E.D., Chiang, L.C., Ma, N., Ortiz de Luna, R.I., Garcia Delgado, C., Gonzalez-Ramos, M., Kline, A.D. and Jabs, E.W. (1997) Mutations in TWIST, a basic helix-loop-helix transcription factor, in Saethre-Chotzen syndrome. Nat Genet 15:36–41.
Kophengnavong, T., Michnowicz, J.E. and Blackwell, T.K. (2000) Establishment of distinct MyoD, E2A, and twist DNA binding specificities by different basic region-DNA conformations. Mol Cell Biol 20:261–272.
Kumar, A., Velloso, C.P., Imokawa, Y. and Brockes, J.P. (2004) The regenerative plasticity of isolated urodele myofibers and its dependence on MSX1. PLoS Biol 2:E218.
Lee, M.S., Lowe, G.N., Strong, D.D., Wergedal, J.E. and Glackin, C.A. (1999) TWIST, a basic helix-loop-helix transcription factor, can regulate the human osteogenic lineage. J Cell Biochem 75:566–577.
Maestro, R., Dei Tos, A.P., Hamamori, Y., Krasnokutsky, S., Sartorelli, V., Kedes, L., Doglioni, C., Beach, D.H. and Hannon, G.J. (1999) Twist is a potential oncogene that inhibits apoptosis. Genes Dev 13:2207–2217.
McGann, C.J., Odelberg, S.J. and Keating, M.T. (2001) Mammalian myotube dedifferentiation induced by newt regeneration extract. Proc Natl Acad Sci USA 98:13699–13704.
Murray, S.S., Glackin, C.A., Winters, K.A., Gazit, D., Kahn, A.J. and Murray, E.J. (1992) Expression of helix-loop-helix regulatory genes during differentiation of mouse osteoblastic cells. J Bone Miner Res 7:1131–1138.
Murre, C., McCaw, P.S. and Baltimore, D. (1989) A new DNA binding and dimerization motif in immunoglobulin enhancer binding, daughterless, MyoD, and myc proteins. Cell 56:777–783.
Odelberg, S.J., Kollhoff, A. and Keating, M.T. (2000) Dedifferentiation of mammalian myotubes induced by msx1. Cell 103: 1099–1109.
Poliard, A., Nifuji, A., Lamblin, D., Plee, E., Forest, C. and Kellermann, O. (1995) Controlled conversion of an immortalized mesodermal progenitor cell towards osteogenic, chondrogenic, or adipogenic pathways. J Cell Biol 130:1461–1472.
Riazi, A.M., Lee, H., Hsu, C. and Van Arsdell, G. (2005) CSX/Nkx2.5 modulates differentiation of skeletal myoblasts and promotes differentiation into neuronal cells in vitro. J Biol Chem 280:10716–10720.
Rosania, G.R., Chang, Y.T., Perez, O., Sutherlin, D., Dong, H., Lockhart, D.J. and Schultz, P.G. (2000) Myoseverin, a microtubule-binding molecule with novel cellular effects. Nat Biotechnol 18:304–308.
Sers, C., Emmenegger, U., Husmann, K., Bucher, K., Andres, A.C. and Schafer, R. (1997) Growth-inhibitory activity and downregulation of the class II tumor-suppressor gene H-rev107 in tumor cell lines and experimental tumors. J Cell Biol 136:935–944.
Shiokawa, D., Kobayashi, T. and Tanuma, S. (2002) Involvement of DNase gamma in apoptosis associated with myogenic differentiation of C2C12 cells. J Biol Chem 277:31031–31037.
Spicer, D.B., Rhee, J., Cheung, W.L. and Lassar, A.B. (1996) Inhibition of myogenic bHLH and MEF2 transcription factors by the bHLH protein Twist. Science 272:1476–1480.
Tajbakhsh, S. (2005) Skeletal muscle stem and progenitor cells: reconciling genetics and lineage. Exp Cell Res 306:364–372.
Thisse, B., Stoetzel, C., Gorostiza-Thisse, C. and Perrin-Schmitt, F. (1988) Sequence of the twist gene and nuclear localization of its protein in endomesodermal cells of early Drosophila embryos. Embo J 7:2175–2183.
van Doorn, R., Dijkman, R., Vermeer, M.H., Out-Luiting, J.J., van der Raaij-Helmer, E.M., Willemze, R. and Tensen, C.P. (2004) Aberrant expression of the tyrosine kinase receptor EphA4 and the transcription factor twist in Sezary syndrome identified by gene expression analysis. Cancer Res 64:5578–5586.
Wang, X., Ling, M.T., Guan, X.Y., Tsao, S.W., Cheung, H.W., Lee, D.T. and Wong, Y.C. (2004) Identification of a novel function of TWIST, a bHLH protein, in the development of acquired taxol resistance in human cancer cells. Oncogene 23:474–482.
Wei, Q. and Paterson, B.M. (2001) Regulation of MyoD function in the dividing myoblast. FEBS Lett 490:171–178.
Yang, J., Mani, S.A., Donaher, J.L., Ramaswamy, S., Itzykson, R.A., Come, C., Savagner, P., Gitelman, I., Richardson, A. and Weinberg, R.A. (2004) Twist, a master regulator of morphogenesis, plays an essential role in tumor metastasis. Cell 117:927–939.

Supplementary material

The following supplementary material is available for this article:

Fig. S1. Efficiency of the Twist antibody on HeLa cells. Twist protein was detected in total (lane 1), nuclear (lane 3), and cytoplasmic (lane 5) extracts from cells transfected with the adenoviral vector (AdT). No Twist was detected in nuclear (lane 2) or cytoplasmic (lane 4) extracts from untransfected cells.

Fig. S2. Quantitative RT/PCR analysis to detect molecular changes in myotubes following their transfection with the Twist gene. Different amounts from the RT were subjected to PCR protocols with a different number of cycles and then plotted in graphs to obtain the linear ranges.

This material is available as part of the online article from: http://www.blackwell-synergy.com/doi/abs/10.1111/j.1432-0436.2007.00195.x (This link will take you to the article abstract).

Please note: Blackwell Publishing is not responsible for the content or functionality of any supplementary materials supplied by the authors. Any queries (other than missing material) should be directed to the corresponding author for the article.

Cell Tissue Res
DOI 10.1007/s00441-007-0439-x

REGULAR ARTICLE

Association of TIMP-2 with extracellular matrix exposed to mechanical stress and its co-distribution with periostin during mouse mandible development

Nagako Yoshiba · Kunihiko Yoshiba · Akihiro Hosoya · Masahiro Saito · Takamasa Yokoi · Takashi Okiji · Norio Amizuka · Hidehiro Ozawa

Received: 21 November 2006 / Accepted: 27 April 2007

Abstract Matrix remodeling is regulated by matrix metalloproteinases (MMPs) and tissue inhibitors of metalloproteinases (TIMPs). Periostin, originally identified in a mouse osteoblastic library, plays a role in cell adhesion and migration and in mechanical stress-induced matrix remodeling. In this study, we analyzed and compared the distribution patterns of TIMP-2 and periostin during mouse mandible development. Immunohistochemical staining for TIMP-2 and periostin was carried out on serial cryosections obtained from mice at embryonic days 13–16, postnatal day 2 (P2), P35, and 12 weeks of age. TIMP-2 and periostin exhibited a strikingly similar protein distribution during mandible development. From bud to early bell stages of molars, TIMP-2 and periostin were highly expressed on the lingual and anterior sides of the basement membrane and on the adjacent jaw mesenchyme. In pre- and postnatal incisors, the basement membrane of the apical loop and dental follicle was immunostained for TIMP-2 and periostin. At postnatal stages, TIMP-2 and periostin were prominently confined to the extracellular matrix (ECM) of gingival tissues, periodontal ligaments, and tendons (all recipients of mechanical strain). However, periostin was solely detected in the lower portion of the inner root sheath of hair follicles. Gingiva of P2 cultured in anti-TIMP-2 antibody-conditioned medium showed markedly reduced staining of periostin. We suggest that TIMP-2 and periostin are co-distributed on ECM exposed to mechanical forces and coordinately function as ECM modulators.

Keywords TIMP-2 · Periostin · Extracellular matrix · Tooth development · Periodontal tissue · Mouse

This work was supported by the Japanese Ministry of Education, Culture, Sports, Science, and Technology and by Niigata University Research Projects.

N. Yoshiba (✉) · K. Yoshiba · T. Okiji
Division of Cariology, Operative Dentistry and Endodontics, Department of Oral Health Science, Niigata University Graduate School of Medical and Dental Sciences,
5274 Gakkocho-dori 2-bancho,
Niigata 951-8514, Japan
e-mail: nagako@dent.niigata-u.ac.jp

A. Hosoya
Department of Oral Histology, Matsumoto Dental University, Shiojiri, Japan

M. Saito
Department of Biochemistry,
Osaka University Graduate School of Dentistry,
Osaka, Japan

T. Yokoi
Department of Medicine, Division of Operative Dentistry and Endodontics, Kanagawa Dental College,
Kanagawa, Japan

N. Amizuka
Center for Transdisciplinary Research, Niigata University,
Niigata, Japan

H. Ozawa
Institute for Dental Science, Matsumoto Dental University,
Shiojiri, Japan

Introduction

Remodeling of the extracellular matrix (ECM) plays a critical role in normal development and in physiological and pathological processes. Matrix metalloproteinases (MMPs) are zinc-dependent proteases capable of degrading all ECM constituents. The activity of these proteases is tightly regulated by actions of tissue inhibitors of metal-

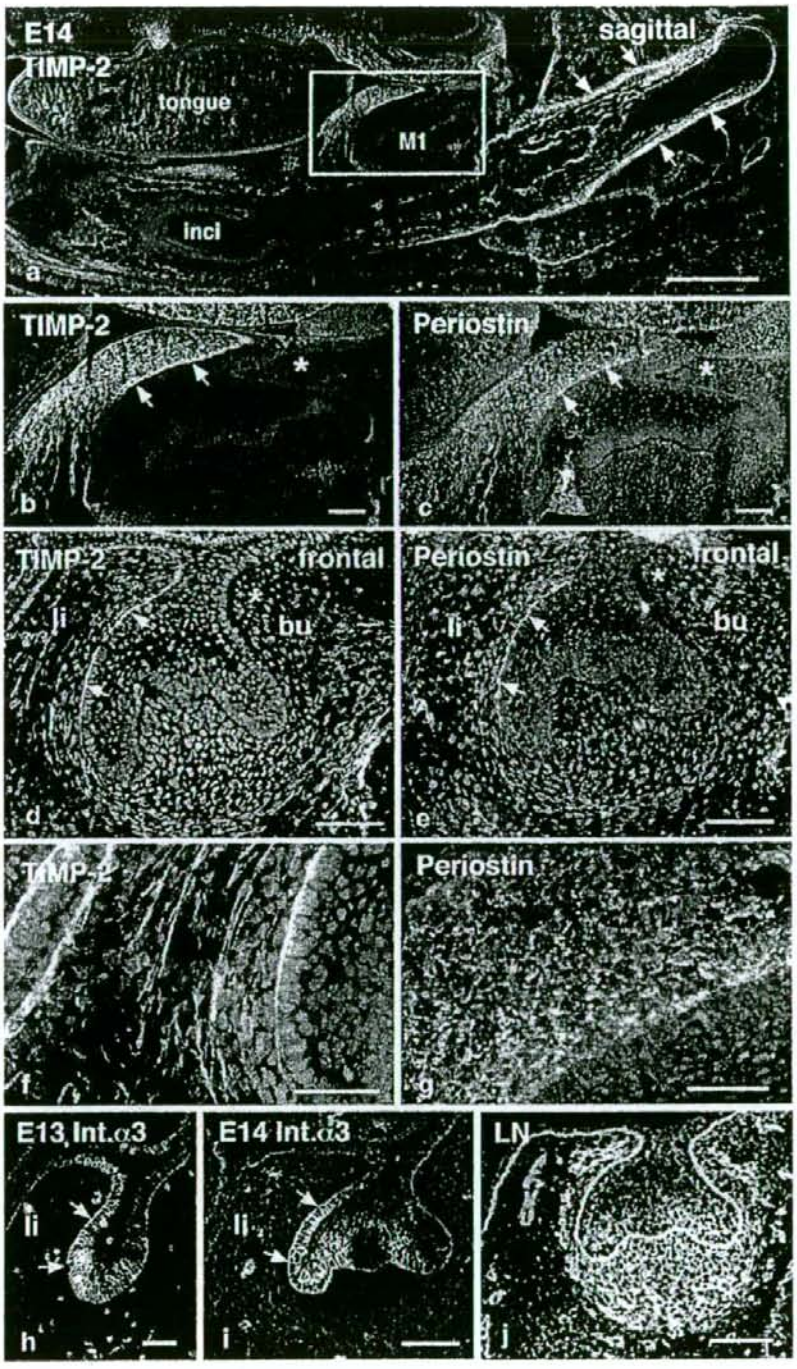
E14
TIMP-2
tongue
M1
sagittal
incl
a
TIMP-2
b
Periostin
c
TIMP-2
frontal
li
bu
d
Periostin
frontal
li
bu
e
TIMP-2
f
Periostin
g
E13 Int.α3
li
h
E14 Int.α3
li
i
LN
j

Fig. 1 Immunohistochemical detection of TIMP-2 and periostin in the mandible at embryonic day (E) 14. **a** Low-power image of a sagittal section of mandible immunostained for TIMP-2. TIMP-2 is restricted to the mandible (*arrows* expression of TIMP-2 on the tendon of Ramus of the mandible, *M1* first molar, *inci* incisor). **b** Higher magnification of *boxed area* in **a**. TIMP-2 is present in the jaw mesenchyme at the anterior part of the molar and along the adjacent basement membrane (*arrows*). In contrast to the anterior region, the posterior part is devoid of TIMP-2 (*asterisk*). **c** Serial section of **b** immunostained for periostin. The tissue distribution of periostin is similar to that of TIMP-2. **d**, **e** Serial frontal sections showing TIMP-2 and periostin expression, respectively. Both proteins are present along the dental basement membrane on the lingual side (*li*) of the molar (*arrows*) and in the adjacent jaw mesenchyme. In contrast, the buccal side (*bu*) is devoid of both proteins (*asterisks*). **f** High-power image of **d** showing that TIMP-2 is associated with ECM. **g** High-power image of **e** demonstrating that periostin lies on the cell surface. **h**, **i** Frontal sections of the molar tooth germ at E13 (**h**) and E14 (**i**) immunostained for integrin α3 (*Int.α3*). Integrin α3 is strongly detected on the lingual side (*li*) of the dental epithelium (*arrows*). **j** Basement membrane of molar germ at E14 labeled for laminin (*LN*) on the frontal section. *Bars* 500 μm (**a**), 100 μm (**b–e**, **h–j**), 50 μm (**f**, **g**)

loproteinases (TIMPs), which are also secreted into the ECM. Efficiencies of MMP inhibition vary among TIMPs, and the balance between MMPs and TIMPs determines the most significant proteolytic events in tissue remodeling. TIMP-2 is ubiquitously expressed as a soluble form in almost every tissue and inhibits various MMPs. TIMP-2 can act as a major inhibitor of membrane-type-1 MMP (MT1-MMP), which is the membrane-anchored-type MMP, and MMP-2. On the other hand, TIMP-2 is essential for the activation of proMMP-2 by MT1-MMP, and excess TIMP-2 completely inhibits the activity of MT1-MMP and activation of proMMP-2 (Seiki 2002). MT1-MMP can digest fibrillar collagen types I, II, and III, and other ECM components including denatured collagen (gelatin), proteoglycans, fibronectin, laminin 1, and vitronectin (Ohuchi et al. 1997). MT1-MMP also activates proMMP-13 (collagenase 13; Knauper et al. 1996a), which degrades fibrillar collagen types I, II, and III (Knauper et al. 1996b). MMP-2 degrades gelatin and collagen types I and IV. In type I collagen-rich stroma, MT1-MMP/MMP-2 seems to act as a potent type I collagen degradation system, and MT1-MMP is highly sensitive to TIMP-2 (Sabeh et al. 2004). In addition to their MMP-inhibitory activity, TIMPs are now widely considered to exert pluripotential effects on cellular behavior such as cell growth, survival, migration, and differentiation, independently of their MMP neutralizing functions (Baker et al. 2002). TIMP-2 can either inhibit (Murphy et al. 1993) or promote (Hayakawa et al. 1994) cell growth. Recently, TIMP-2 has been shown to be the ligand of integrin α3β1, and ligand binding directly inhibits the proliferation of endothelial cells (Seo et al. 2003). Of the four known TIMPs, TIMP-2 has been thought to be soluble and not to bind to ECM, in contrast to TIMP-3 (Yu et al. 2000). However, our previous data have indicated that TIMP-2 also binds to ECM in a peculiar distribution pattern during tooth development in mouse from embryonic day (E)13 to postnatal day (P)3 (Yoshiba et al. 2003, 2006).

Teeth are formed from ectoderm-derived oral epithelial and neural-crest-derived ectomesenchymal cells. The dental epithelium invaginates into the mesenchyme and forms the tooth bud (E13), cap (E14), and the bell (E16), at which time the shape of the tooth crown is established. The epithelium then gives rise to enamel. The condensed mesenchyme forms the dental papilla and dental follicle, which give rise to odontoblasts, cementoblasts, periodontal ligaments, and alveolar bone. Continuously erupting incisors of rodents contain a stem cell compartment (the apical loop) at the apical end, which consists of stem cells for all types of epithelia of incisors. From the bud to early bell stages of molar tooth development, TIMP-2 has been shown to be associated with the ECM in the jaw mesenchyme on the lingual side of the molar germ and along the lingual side of the dental basement membrane (Yoshiba et al. 2003). At P3, TIMP-2 accumulates on both sides of the molar germ (Yoshiba et al. 2003). During incisor development (E14-P3), TIMP-2 is restricted to the basement membrane of the apical loop. In contrast to the restricted localization of TIMP-2, *Timp-2* mRNA is broadly expressed (Yoshiba et al. 2003, 2006).

Periostin is an ECM protein that was originally isolated from an osteoblastic cell line and was first known as osteoblast-specific factor 2 (Osf-2; Takeshita et al. 1993). Thereafter, Osf-2 was renamed to periostin, because of its preferential expression in the periosteum and periodontal ligaments; it has been reported to support osteoblastic cell attachment and spreading (Horiuchi et al. 1999). Periostin is highly homologous to βig-h3, previously known as transforming growth factor-β (TGF-β)-inducible protein. Both periostin and βig-h3 contain fasciclin (Fas-1) domains (Takeshita et al. 1993; Skonier et al. 1994). The Fas-1 domains of βig-h3 have been shown to interact with integrin α3β1 of epithelial cells (Kim et al. 2000) and with integrin αvβ5 of mesenchymal cells (Kim et al. 2002). Thus, Fas-1 domain-containing proteins are suggested to perform their biological functions by interacting with integrins (Kim et al. 2002). On the other hand, periostin has also been shown to mediate cell adhesion by binding to integrins αvβ3 and αvβ5 (Gillan et al. 2002). Furthermore, periostin is suggested to bind to integrin α3β1, because of the existence of suitable binding sites in Fas-1 domains (Kudo et al. 2004). Recently, two laboratories have generated *periostin* null mice (Rios et al. 2005; Kii et al. 2006). These null mice have abnormal postnatal incisors, suggesting the critical requirement of periostin for the integrity of periodontal ligaments in response to mechanical stresses (Rios et al. 2005) and its function in the remodeling of the collagen matrix in the shear zone (Kii et al. 2006). In addition to their localization in

periodontal ligaments, periostin mRNA and protein have been shown to be present at higher levels on the lingual side of the mouse molar tooth germ compared with the buccal side (Kruzynska-Frejtag et al. 2004), and the surface of the apical loop in postnatal mouse incisors shows weak positive reactivity for periostin (Suzuki et al. 2004). Although the localization of periostin has not been fully analyzed during molar and incisor tooth morphogenesis, the reported localization of periostin is intriguingly similar to that of TIMP-2 mentioned above. *Timp-2* mRNA is expressed in periodontal ligaments and in tendons. However, whether TIMP-2 can associate with ECM in these tissues remains unknown.

In order to test the hypothesis that TIMP-2 can associate with ECM of specific areas and co-distribute with periostin, we have analyzed the tissue distribution patterns of TIMP-2 and periostin in mouse mandible development by using immunohistochemistry. Furthermore, the dissected mandible has been cultured in the presence of anti-TIMP-2 antibody, and the localization of periostin has been evaluated.

Materials and methods

Preparation of tissues

Heads of mouse embryos at E13–E16 and P2 were embedded in Tissue-Tek O.C.T. Compound (SAKURA), frozen in liquid nitrogen, and cut as 8-μm-thick frontal or sagittal sections. Lingual gingival tissues of adult mice were isolated, and cryosections were prepared as described above. Mandibles at P35 and P12 weeks were also frozen, and cryosections were prepared.

Indirect immunofluorescence

Immunostaining with antibodies raised against periostin (1:50 dilution; BioVender, Heidelberg, Germany), TIMP-1 (1:100 dilution; R&D Systems, Minneapolis, Minn.), TIMP-2 (1:100 dilution; Chemicon, Temecula, Calif.), TIMP-3 (1:100 dilution; Chemicon), laminin (1:400; Sigma, St. Louis, Mo.), and integrin α3 (1:400 dilution; BD, N.J.) was performed on cryosections as previously described (Yoshiba et al. 2003). Briefly, cryosections were fixed in cooled acetone, washed in phosphate-buffered saline (PBS), and incubated with the primary antibodies followed by Cy3-conjugated secondary antibodies (1:500 dilution; Jackson Immunoresearch, West Grove, Pa.).

In situ hybridization

TIMP-2 cDNA (Leco et al. 1992) was kindly provided by Dr. Robert Nuttall (University of East Anglia, Norfolk, UK). The [^{35}S]CTP-labeled sense and antisense riboprobes were prepared by in vitro transcription. In situ hybridization on cryosections was performed as described previously (Yoshiba et al. 2003).

Organ culture experiments

Gingival tissue with the associated molar was dissected from the mandible at P2 and cultured for 4 days in serum-free DMEM supplemented with penicillin/streptomycin. For antibody inoculation, anti-TIMP-2 antibody was added to the culture medium at a concentration of 50 μg/ml. Antibodies against TIMP-1 and TIMP-3 were used as controls at the same concentration. The cultured tissue was embedded in Tissue-Tek, and cryosections were prepared. Immunofluorescence was performed as described above.

Results

Localization of TIMP-2 and periostin in mandible at E14

TIMP-2 was localized in specific areas of sagittal sections of mandibles at E14 (Fig. 1a). Pronounced immunoreaction of TIMP-2 was observed in the jaw mesenchyme at the anterior part of the molar (Fig. 1a, b) and in the tendon of Ramus of the mandible (Fig. 1a, arrows). Intriguingly, in sagittal serial sections, periostin showed the same distribution pattern as TIMP-2. The jaw mesenchyme at the anterior part of the molar was abundant in periostin (Fig. 1c). In contrast, the posterior part of the molar was devoid of both proteins (Fig. 1b, c, asterisks). In serial frontal sections, TIMP-2 and periostin were found to be present along the dental basement membrane on the lingual side of the molar and on the adjacent jaw mesenchyme (Fig. 1d, e). In contrast, the jaw mesenchyme on the buccal side was devoid of both proteins (Fig. 1d, e, asterisks). TIMP-2 appeared to associate with the ECM (Fig. 1b, d, f). On the other hand, periostin was observed on the cell surface (Fig. 1g). TIMP-2 has been reported to bind to integrin α3 (Seo et al. 2003), and periostin has been suggested to be a ligand of integrin (Kudo et al. 2004). Hence, the localization of integrin α3 was analyzed. Integrin α3 was readily recognized on the lingual side of the dental epithelium at E13 (Fig. 1h) and E14 (Fig. 1i), and its reactivity decreased at E16 (data not shown). The localization pattern of integrin α3 was in agreement with those of TIMP-2 and periostin on the basement membrane.

Localization of TIMP-2 and periostin in mandible at E16

TIMP-2 and periostin showed the same distribution patterns at E16. Both proteins were localized in tendons (Fig. 2a, c, d), but their staining patterns were different (Fig. 2c, d). On

the molar germ at the bell stage, TIMP-2 (Fig. 2e) and periostin (Fig. 2f) disappeared from the basement membrane, except on the lingual side of the dental lamina. In the jaw mesenchyme, both proteins were detected on the lingual side, the buccal side being devoid of TIMP-2 and periostin (Fig. 2e, f, asterisks). Detailed analysis revealed that TIMP-2 was apparently associated with the ECM in the jaw mesenchyme (Fig. 2g), whereas periostin demonstrated a punctate pattern combined with fine fibrils (Fig. 2h).

Localization of TIMP-2 and periostin in gingival tissues at P2 and in adult mice

TIMP-2 (Fig. 3a) and periostin (Fig. 3b) accumulated in the jaw mesenchyme on both sides of the molar germ at P2 in an area that corresponded to future gingival tissues. They were present on the ECM and on fibers connecting to the alveolar bone (Fig. 3d, e, arrows). In adult mice, TIMP-2 remained accumulated in gingival tissues (Fig. 3f). Periostin was also abundantly detected in gingival tissues (data not shown). TIMP-3 has been suggested to be an ECM-binding protein. Hence, we analyzed the localization of TIMP-3 and TIMP-1 in adult gingival tissues. In contrast to TIMP-2, neither TIMP-1 (Fig. 3g) nor TIMP-3 (Fig. 3h) was restricted to gingival tissues. To support the immunohistochemical results with respect to TIMP-2, the expression of *Timp-2* mRNA was analyzed at P2. *Timp-2* was strongly expressed in the periodontal tissues, including the periodontal ligaments (Fig. 3j, arrows) and gingival tissues (Fig. 3k).

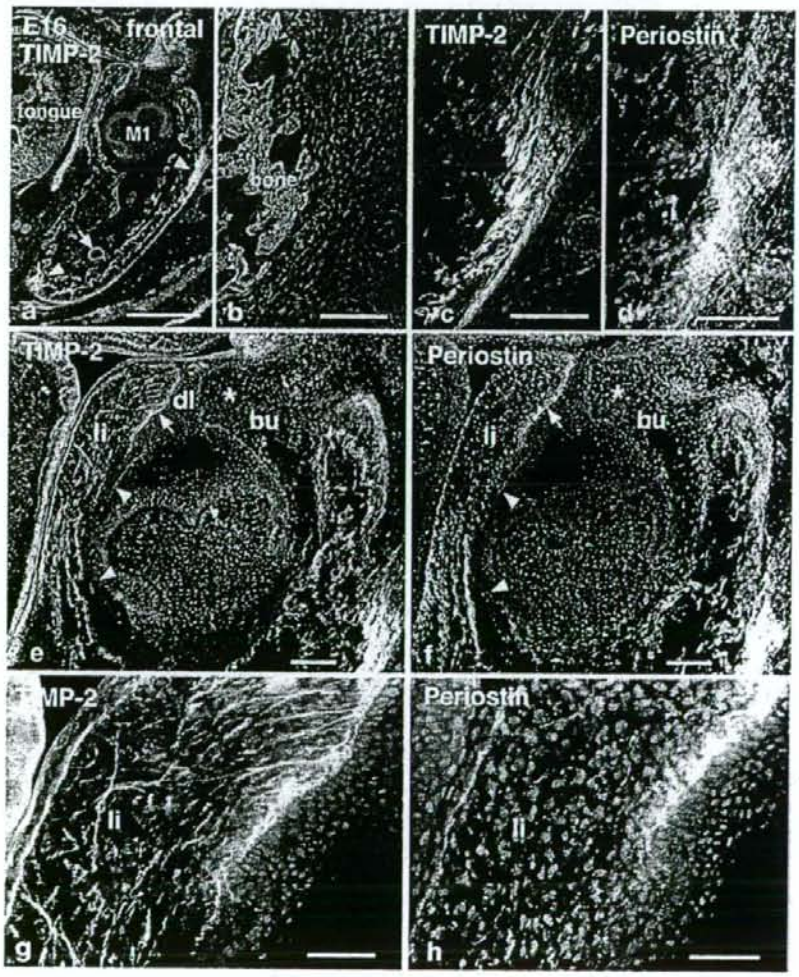

Fig. 2 Immunohistochemical detection of TIMP-2 and periostin in the mandible at E16. **a** Low-power image of a frontal section of the mandible stained with TIMP-2 (*arrowheads* expression of TIMP-2 in the tendon, *arrow* expression of TIMP-2 on basement membrane of apical loop of incisor). **b–d** A higher power image of the area indicated by the *arrowhead* (*right*) in **a** is presented in **c**, and its phase-contrast image is shown in **b**. **d** Serial section to that in **c** immunostained for periostin. TIMP-2 (**c**) and periostin (**d**) distribution patterns are similar. **e, f** Serial frontal sections showing TIMP-2 and periostin expression, respectively. Both proteins disappear from the basement membrane on the lingual side (*li, arrowheads*), although they are detectable along the dental lamina (*dl*) on the lingual side (*arrow*). In the jaw mesenchyme, both proteins are localized on the lingual side; in contrast, the buccal side (*bu*) is devoid of TIMP-2 and periostin (*asterisks*). **g, h** Higher power views of the lingual jaw mesenchyme of **e, f**, respectively. *Bars* 500 μm (**a**), 100 μm (**b–f**), 50 μm (**g, h**)

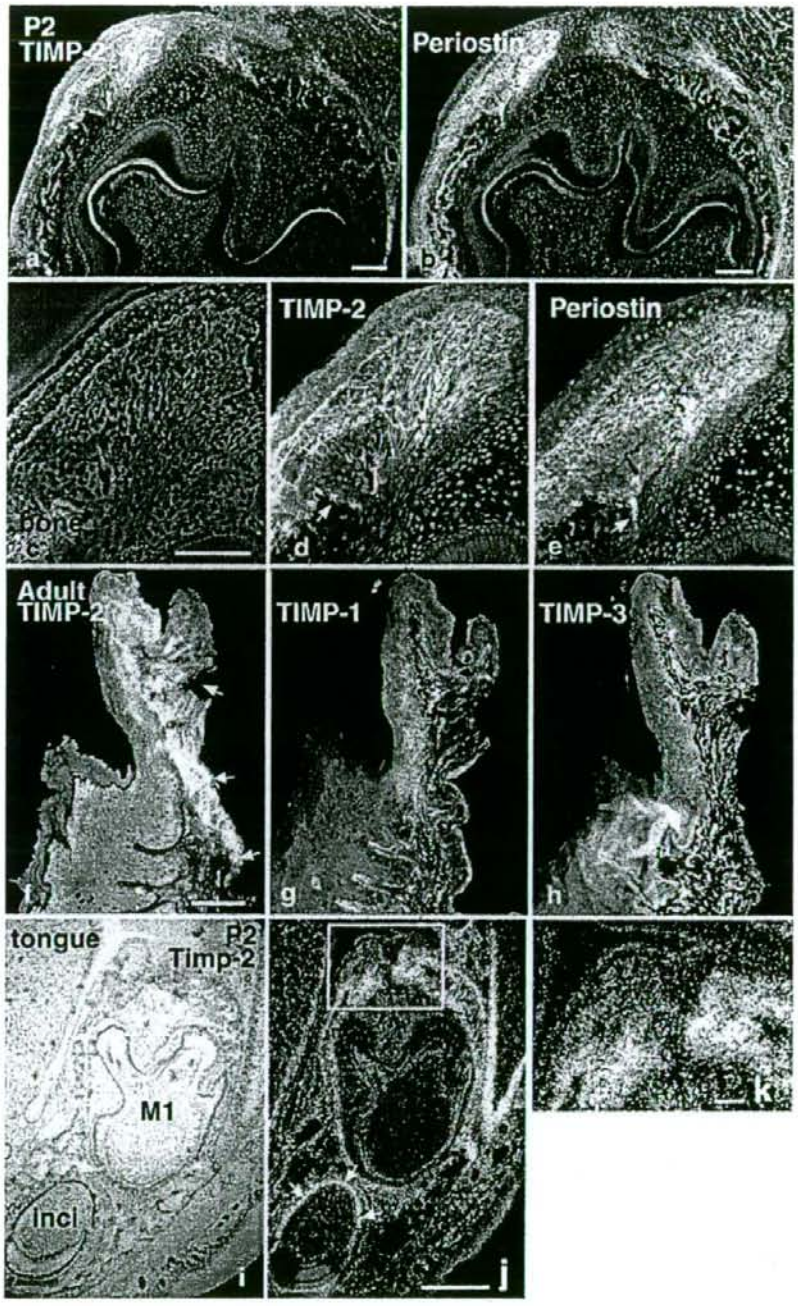
P2
TIMP
a
Periostin
b
bone
c
TIMP-2
d
Periostin
e
Adult
TIMP-2
f
TIMP-1
g
TIMP-3
h
tongue
P2
Timp-2
M1
Incl
i
j
k

Fig. 3 Immunohistochemical detection of TIMP-2 and periostin in gingival tissues at postnatal day 2 (P2) and in adult mouse, and in situ hybridization analysis of TIMP-2 at P2. **a**, **b** Serial frontal sections stained with TIMP-2 and periostin, respectively. The jaw mesenchyme is strongly stained with TIMP-2 and periostin on both sides of the molar germ at P2. **c–e** High-power images of **a**, **b** are presented in **d**, **e**, respectively; **c** is the phase-contrast image of **d**. Although both proteins are visible on the ECM, their staining patterns are different. Fibers connecting to alveolar bone are also stained with both proteins (**d**, **e**, *arrows*). **f–h** TIMP-2 is strongly detected in gingiva of adult mouse (**f**, *arrows*). In contrast, neither TIMP-1 (**g**) nor TIMP-3 (**h**) is restricted to gingival tissues. **i–k** In situ hybridization analysis of TIMP-2 at P2. **i** Bright-field image of **j** (*M1* first molar, *inci* incisor). **k** Higher power view of *boxed area* in **j**. *Timp-2* transcripts are detected in the periodontal ligament (**j**, *arrows*) and gingival tissue (**k**). *Bars* 500 μm (**j**), 100 μm (**a–c**, **f**, **k**)

Localization of TIMP-2 in periodontal ligament at P35 and 12 weeks

The periodontal ligament is a soft connective tissue that serves to anchor the tooth to the alveolar bone and functions as a cushion between two mineralized tissues. Expression of periostin is temporospatially regulated in the periodontal ligament, which is broadly stained with periostin at P21 in mouse (Suzuki et al. 2004).

Hence, the localization of TIMP-2 was analyzed in periodontal ligaments. In frontal sections of mandibles at P35, strong TIMP-2 immunoreactivity was partially seen in periodontal ligaments (Fig. 4a, arrows). TIMP-2 was strongly detected on the alveolar bone or cementum side

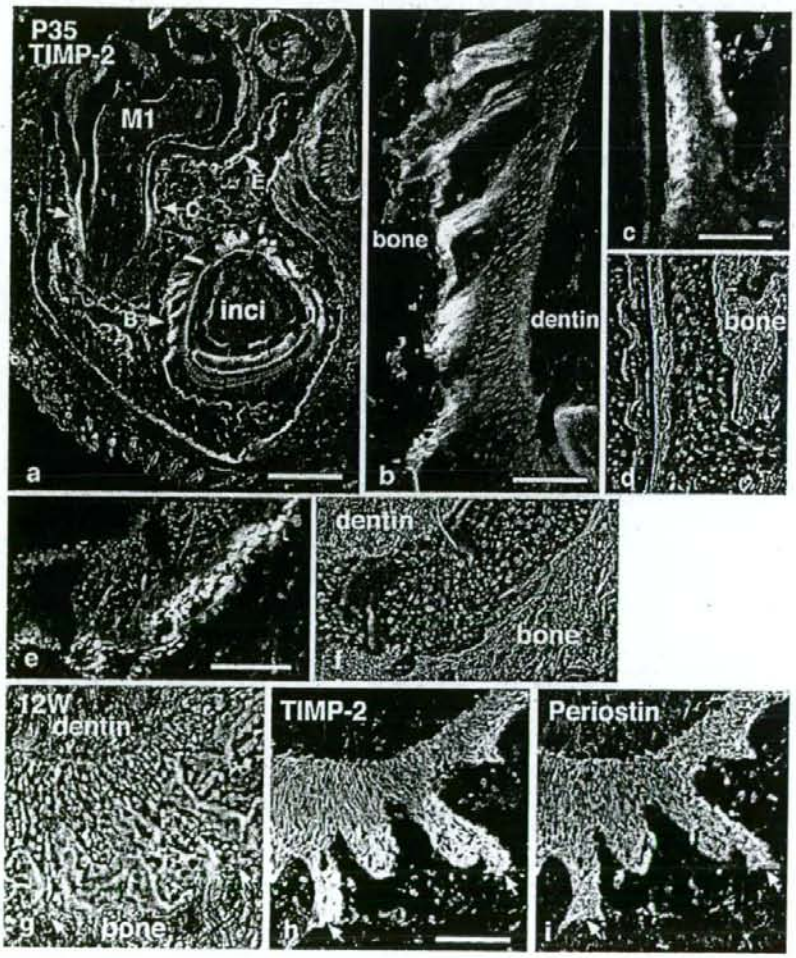

Fig. 4 Immunohistochemical detection of TIMP-2 in the periodontal ligament at P35 and 12 weeks of age. **a** Low-power image of a frontal section of mandible stained with TIMP-2 (*arrows* expression of TIMP-2 in the periodontal ligament of the molar and incisor, *M1* molar, *inci* incisor). **b–f** High-power images of the areas indicated as *B*, *C*, *E* in **a** are shown in **b**, **c**, **e**, respectively. **d**, **f** Phase-contrast images of **c**, **e**, respectively. A part of the periodontal ligament is strongly stained with TIMP-2. **g–i** A phase-contrast image of **h** is presented in **g**. TIMP-2 (**h**) and periostin (**i**) are broadly detected in the periodontal ligament at 12 weeks of age (*arrows* junctions between the ligament and alveolar bone). *Bars* 500 μm (**a**), 100 μm (**b–h**)

of the ligament (Fig. 4b, c, e). TIMP-2 was broadly observed in the periodontal ligament at 12 weeks (Fig. 4h) and thus had a distribution similar to that of periostin (Fig. 4i).

Localization of TIMP-2 and periostin in mandibular joint at P2

In order to confirm that TIMP-2 associated with the ECM of tendons, the mandibular joint at P2 was analyzed. TIMP-2 (Fig. 5c, e) and periostin (Fig. 5g, h) were similarly distributed in this tissue. TIMP-2 was clearly immunostained in the ECM of the tendon (Fig. 5e, arrows). In contrast, the ECM of the tendon was devoid of TIMP-3 (Fig. 5f, arrows). To support the immunohistochemical results of TIMP-2 expression, the expression of *Timp-2* mRNA was analyzed. *Timp-2* transcripts were detectable in the tendon (Fig. 5a, b, arrows).

Localization of TIMP-2 and periostin during incisor development

The temporospatial distribution of TIMP-2 and periostin was similar and specific during molar tooth development. The distribution patterns of TIMP-2 and periostin were further examined during incisor tooth development. The basement membrane of the incisor was initially devoid of both TIMP-2 and periostin at E13 (bud stage, data not shown). At the early bell stage of E14, TIMP-2 was weakly expressed on the basement membrane of the apical loop, whereas periostin was negligibly detected at this position and at this stage (data not shown). At the bell stages of E16 and P2 (Fig. 6c), periostin was detectable on the basement membrane of the apical loop, in addition to TIMP-2 (Fig. 6b). Both proteins could also be recognized in the dental follicle (Fig. 6b, c). Detailed inspection of the basement membrane and the dental follicle revealed differences in immunostaining patterns of periostin and TIMP-2 (Fig. 6d, e).

Localization of TIMP-2 and periostin in skin at P2

TIMP-2 and periostin asymmetrically colocalized on the dental basement membrane during tooth development. The basement membrane of skin (also exposed to mechanical force) was additionally analyzed. TIMP-2 and periostin colocalized along the basement membrane of the epidermis and the upper part of the outer root sheath of hair follicles (Fig. 7b, c, double arrows). Unexpectedly, periostin was solely detected on the lower portion of the inner root sheath (Fig. 7c, arrows). The upper part of the inner root sheath was devoid of periostin (Fig. 7c, arrowheads).

Loss of periostin immunoreactivity in gingiva cultured with anti-TIMP-2 antibody

TIMP-2 and periostin were significantly co-distributed in vivo. Therefore, we investigated their functional relationships in vitro. As TIMP-2 and periostin were abundantly

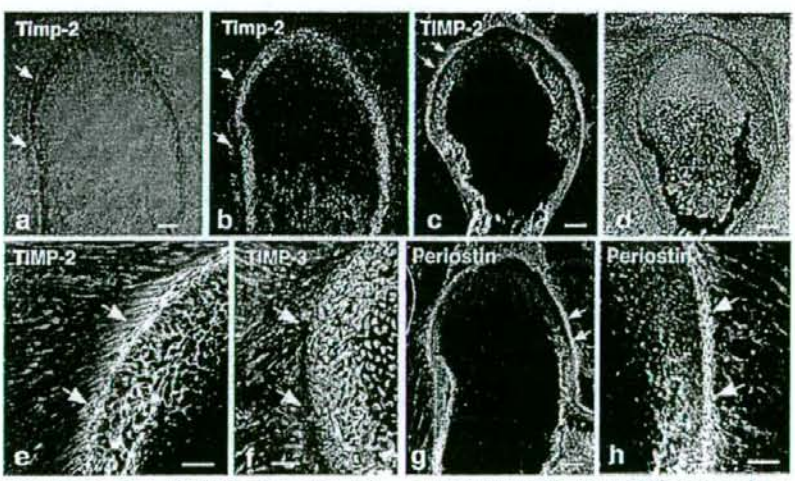

Fig. 5 Immunohistochemical detection of TIMP-2 and periostin, and in situ hybridization analysis of TIMP-2 in the mandibular joint at P2. **a, b** In situ hybridization analysis of TIMP-2. **a** Bright-field image of **b**. *Timp-2* transcripts are detected in tendons (*arrows*). **c–e** TIMP-2 protein localization in the mandibular joint. **d** Phase-contrast image of **c**. **e** Higher power view of the area indicated by *arrows* in **c**. TIMP-2 protein is associated with the ECM of the tendon (**e**, *arrows*). **f** TIMP-3 is not detected in the ECM of the tendon (*arrows*). **g** Low-power image of immunostaining for periostin. **h** Higher power view of the area indicated by *arrows* in **g**. Periostin is localized on the tendon (**h**, *arrows*). *Bars* 100 μm (**a**, **c**, **d**, **g**), 50 μm (**e**, **f**, **h**)

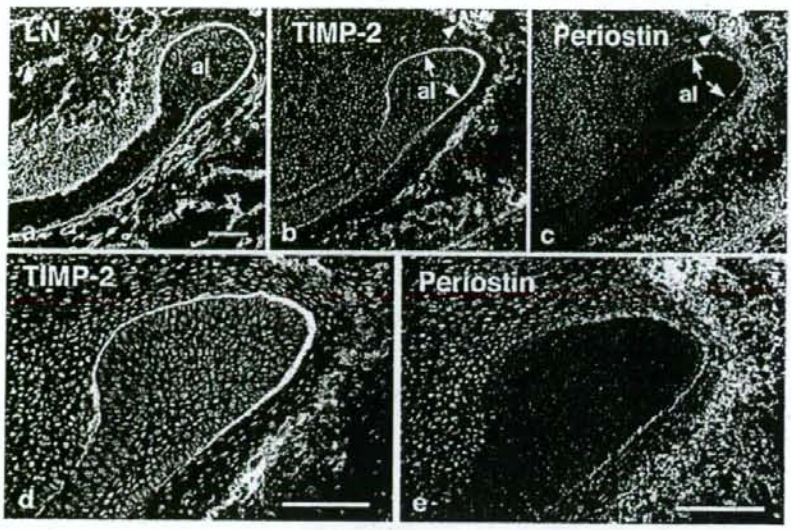

Fig. 6 Immunohistochemical detection of TIMP-2 and periostin in the incisor at P2. **a** Labeling of the basement membrane of the incisor for laminin (*LN*). **b**, **c** TIMP-2 (**b**) and periostin (**c**) are restricted to the basement membrane of the apical loop (*al*, *arrows*) and to the dental follicle (*arrowhead*). **d**, **e** High-power images of **b**, **c**, respectively. Immunostaining patterns are different between TIMP-2 and periostin. *Bars* 100 μm

present on the ECM of gingival tissues at P2 (Fig. 3a, b), gingiva at P2 was dissected with the molar germ,and cultured for 4 days with or without anti-TIMP-2 antibody. In the absence of anti-TIMP-2 antibody, the ECM of the cultured gingiva was strongly positive for TIMP-2 (Fig. 8a) and periostin (Fig. 8b). Neutralization of TIMP-2 with anti-TIMP-2 antibody resulted in a loss of staining of periostin in the gingiva (Fig. 8c, d). The specificity of the anti-TIMP-2 antibody effect on periostin was demonstrated by culturing gingiva with anti-TIMP-1 or anti-TIMP-3 antibody. Periostin could still be localized in anti-TIMP-1-treated (Fig. 8e, f) and anti-TIMP-3-treated (Fig. 8g, h) tissues.

Discussion

In this study, we have demonstrated that TIMP-2 protein coexists with the ECM of specific tissues, e.g., gingiva, periodontal ligaments, and tendons, which are all constantly exposed to mechanical forces. Furthermore, TIMP-2 is asymmetrically localized on the dental basement membrane. The tissue distribution of TIMP-2 is temporospatially regulated and corresponds remarkably to that of periostin.

Both TIMP-2 and periostin are secreted proteins and seem to be associated with the ECM. However, their abilities to bind to ECM components seem to be inconsis-

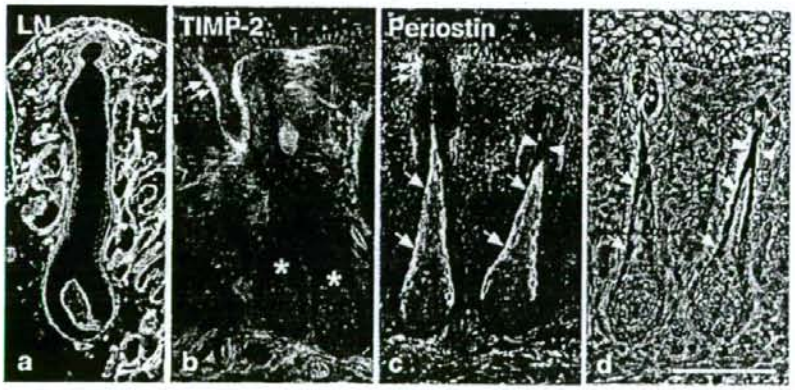

Fig. 7 Immunohistochemical detection of TIMP-2 and periostin in skin at P2. **a** Labeling of the basement membrane of the hair follicle for laminin (*LN*). **b** TIMP-2 is present on the basement membrane of the epidermis and the upper part of the outer root sheath of the hair follicle (*double arrow*). The lower part of the hair follicle is devoid of TIMP-2 (*asterisks*). **c**, **d** A phase-contrast image of **c** is shown in **d**. Periostin is also present on the basement membrane of the epidermis and the upper part of the outer root sheath of the hair follicle (*double arrow*). Notably, periostin is solely detected on the lower portion of the inner root sheath (*arrows* in **c**). The upper part of the inner root sheath is devoid of periostin (**c**, *arrowheads*). *Bar* 100 μm